Thermal Conductivity of Gaseous 1,1,1,2,3,3,3-Heptafluoropropane (HFC-227ea)

Xiao-Jun Liu, Lin Shi,* Yuan-Yuan Duan, Li-Zhong Han, and Ming-Shan Zhu

Department of Thermal Engineering, Tsinghua University, Beijing 100084, P. R. China

The thermal conductivity of gaseous 1,1,1,2,3,3,3-heptafluoropropane (HFC-227ea) is reported over the temperature range from 13.87 to 68.58 °C at pressures up to 1.289 MPa. A transient hot-wire instrument with two anodized tantalum wires was used as the heat source. The uncertainty of the results is estimated to be less than ±3%. The results are correlated as a function of temperature and density. The thermal conductivity of the dilute gas and the saturated vapor are obtained by extrapolation.

Introduction

The expected worldwide ban on many common chlorofluorocarbon (CFC) and hydrochlorofluorocarbon (HCFC) products has prompted a vigorous search for alternatives with zero ozone-depletion potential (ODP) and lower global warming potential (GWP). HFC-227ea (1,1,1,2,3,3,3-heptafluoropropane) has zero ODP. It is useful in fire suppression, refrigeration, sterilization, and propellant applications. It has been used as an alternative to Halon. Mixtures containing HFC-227ea were developed as potential alternatives to HCFC-22 and R502. Effective use of HFC-227ea requires that the thermodynamic and transport properties be accurately measured, but there are very little data available, especially for the transport properties. Robin (1994) listed the thermophysical properties of HFC-227ea including estimated transport properties on the basis of experimental data of Salvi-Narkhede et al. (1992). Huber et al. (1996) developed a database, REFPROP, to calculate the thermophysical properties of refrigerants and refrigerant mixtures, which can be used to estimate the thermal conductivity of HFC-227ea along the saturation line. But no reliable experimental data for the thermal conductivity of gaseous HFC-227ea has been published, so research on the thermal conductivity of HFC-227ea is of great interest.

In this paper, the thermal conductivity of gaseous HFC-227ea was measured with a transient hot-wire instrument at temperatures between −13.87 and 68.58 °C and pressures up to 1.289 MPa. The uncertainty of the results is estimated to be less than ±3%.

Working Equation

Healy et al. (1976) described the theoretical basis for the transient hot-wire technique for gas thermal conductivity measurement. According to the theory, the thermal conductivity of the fluid can be obtained with the following equation

$$\Delta T_{id} = \Delta T_w + \Sigma \delta T_i = \frac{q}{4\pi\lambda(T_r, \rho_r)} \ln\frac{4Fo}{C} \qquad (1)$$

in which

$$T_r = T_0 + \frac{1}{2}(\Delta T_1 + \Delta T_2) \qquad (2)$$

* To whom correspondence should be addressed. E-mail: lshi@te.tsinghua.edu.cn.

where ΔT_{id} is the temperature increase of the hot-wire under ideal conditions; ΔT_w is the temperature increase of the hot-wire under the experimental conditions; δT_i are various correction terms; T_r is the reference temperature; ρ_r is the density of the fluid at the reference temperature T_r and the primary pressure P_0, λ is the thermal conductivity of the fluid at temperature T_r and pressure P_0; Fo is the Fourier number ($Fo = k\tau/a^2$), where k is the thermal diffusivity of the fluid surrounding the wires, τ is the heating time, and a is the wire radius; and C is a numerical constant, $C = 1.781\cdots\cdots$. T_0 is the equilibrium temperature of the fluid before heating, and ΔT_1 and ΔT_2 are the temperature increases of the hot-wire at the beginning and the end of the temperature measurement period, respectively.

The various correction terms, δT_i, were identified (Healy et al., 1976) and all are rendered less than ±1% of ΔT_{id} except the correction term induced by the thermophysical properties of the hot-wire. When the heat capacities of the fluid and the wires are not the same and the heat transfer coefficient of the wires is limited, Joschke (1977) suggested that the real temperature increase could be expressed as

$$\Delta T = \frac{q}{4\pi\lambda}\left[2h + \ln\frac{4Fo}{C} - \frac{4h - W}{2WFo} + \frac{W - 2}{2WFo} \times \ln\frac{4Fo}{C} + \cdots\cdots\right] \qquad (3)$$

where ΔT is the real temperature increase; $h = 2\pi\lambda/H$, where H is the heat transfer coefficient of the wire to the fluid surrounding the wires; $w = 2(\rho_f \times Cp_f)/(\rho_w \times Cp_w)$, where $\rho_f \times Cp_f$ and $\rho_w \times Cp_w$ are the heat capacities of the fluid and the wires, respectively. Ignoring the effect of H and only considering the effect of the heat capacity of the wire, eq 3 can be rewritten as

$$\Delta T = \frac{q}{4\pi\lambda}\left[\ln\frac{4Fo}{C} + \frac{1}{2Fo} + \frac{W - 2}{2WFo} \times \ln\frac{4Fo}{C} + \cdots\cdots\right] \qquad (4)$$

When eq 1 and eq 4 are compared, ΔT_{id} can be calculated with eq 5:

$$\Delta T_{id} = K\Delta T = \frac{\ln\frac{4Fo}{C}}{\ln\frac{4Fo}{C} \times \left(1 + \frac{W - 2}{2WFo}\right) + \frac{1}{2Fo}}\Delta T \qquad (5)$$

10.1021/je9802625 CCC: $18.00
Published on Web 06/30/1999

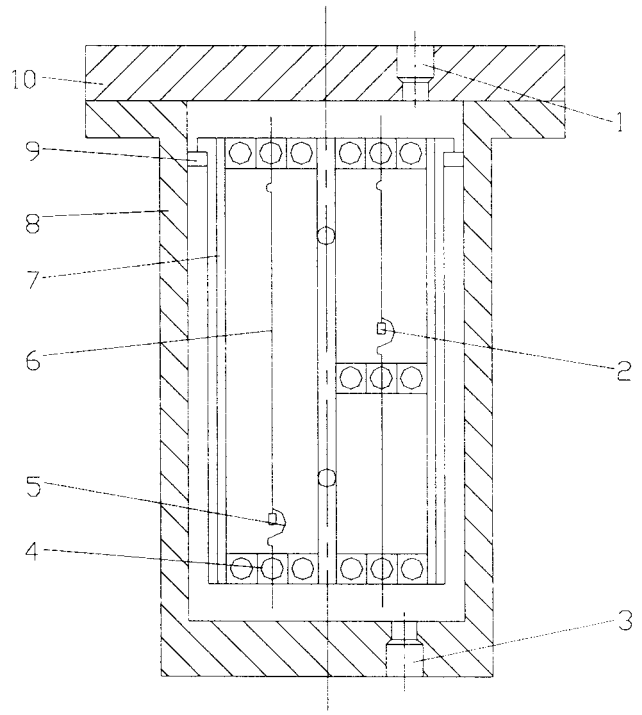

Figure 1. Instrument schematic. 1: Holes for wire extension; 2: copper block; 3: test fluid charging hole; 4: mount for wires; 5: gold strip; 6: tantalum wire; 7: copper compartment, 8: pressure vessel; 9: aluminum ring; 10: flange plate.

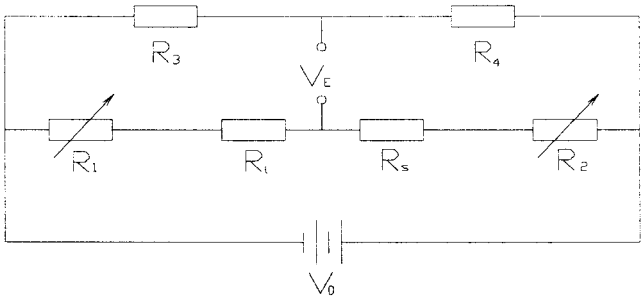

Figure 2. Unbalanced bridge for measuring wire resistance.

From eq 1, an essential feature of the correct operation of the instrument is that the measured ΔT_{id} should be a linear function of the logarithm of τ. Once the temperature increase of the hot-wire is measured as a function of time, the gradient of the linear function of ΔT versus the logarithm of τ can be used to calculate the original thermal conductivity of the fluid around the hot-wire. Then, using eq 5, the temperature increases can be corrected. With the same theory, a new set of thermal conductivity data can be obtained, which reduces the effect of the heat capacity of the hot-wire.

Instrumentation

The thermal conductivity instrument used in this work was previously described in detail (Sun et al., 1997; Duan et al., 1997). The cut-away view of the cylinder is shown in Figure 1.

The instrument uses two 25 μm tantalum wires as hot-wires to eliminate the errors caused by the finite length (Kestin and Wakeham, 1978). The wires were anodized to form a layer of insulating tantalum pentoxide on their surfaces. All electrical connections to the hot-wires were made of 0.8 mm diameter enamel-insulated copper wire which extended outside of the pressure vessel. The tantalum wires were kept vertical and under constant tension by a copper block attached to the bottom of each wire. The mass of the copper blocks was chosen to keep the tension of hot-wires at 25% of their yielding strength (Menashe and Wakeham, 1981). The wires were very carefully connected to eliminate contact resistant in the measurement system.

The wires were carefully calibrated to determine the resistance temperature coefficient of the tantalum wire. The tantalum wire resistance, $R(\Omega)$, was represented as a polynomial function of the temperature t over the temperature range from −15 to 70 °C. A least-squares analysis of the data yielded

$$R(t) = R_0[1 + 3.6314 \times 10^{-3}(t/°C) - 5.46806 \times 10^{-6}(t/°C)^2] \quad (6)$$

where R_0 represents the resistance of the hot-wires at the temperature of 0 °C.

The resistance changes caused by the temperature increase of the wires were measured with an unbalanced bridge, Figure 2. With this bridge, the difference between the resistance of the two wires can be written in the following form by assuming that the two wires are identical except for their length.

$$\Delta R = R_l - R_s = \left(\frac{l_l}{l_s} - 1\right)\frac{CR_1 + CR_2 - R_1}{\frac{l_l}{l_s}(1 - C) - C} \quad (7)$$

in which

$$C = \frac{V_E}{V_o} + \frac{R_3}{R_3 + R_4} \quad (8)$$

where R_l is the resistance of the long hot-wire; R_s is the resistance of the short hot-wire; l_l is the length of the long wire; l_s is the length of the short wire; R_1 and R_2 are the resistance of two adjustable resistors; V_0 is the voltage of the power source; V_E is the measured voltage across the bridge; and R_3 and R_4 are the resistance of two standard fixed resistors. Resistors R_1 and R_2 were carefully chosen to ensure a uniform energy input in the experiment. The bridge voltage V_E was measured with a Hewlett-Packard 3852A data acquisition unit at a collecting rate of about 30 points/s. The temperature increase of the hot-wires was about 2 to 4 °C in the experiment. The instrument uncertainty was estimated to be less than ±3%.

The pressure measurement system included a piston-type pressure gauge, a pressure transducer, and an atmospheric pressure gauge. The accuracy of the piston-type pressure gauge was less than 0.005% in the range 0.1 to 6 MPa. A very sensitive, diaphragm pressure transducer (405T) separated the sample from a nitrogen-filled system, which was connected with the precision piston-type pressure gauge. The accuracy of the transducer was 0.2%, the pressure difference was adjusted over the range 6−38 kPa, the temperature range was 233−400 K, and the maximum allowable pressure was 17.8 MPa. The accuracy of the atmospheric pressure gauge was 0.05% over a pressure range of 1−160 kPa. The whole pressure measurement system had an uncertainty of ±500 Pa.

The bath temperature could be varied from 223 to 452 K. The temperature instability was less than ±5 mK per 8 h. The overall temperature uncertainty for the bath and temperature measurement system was less than ±10 mK.

The instrument was tested by Duan et al. (1997) by comparing measured values of the thermal conductivity of

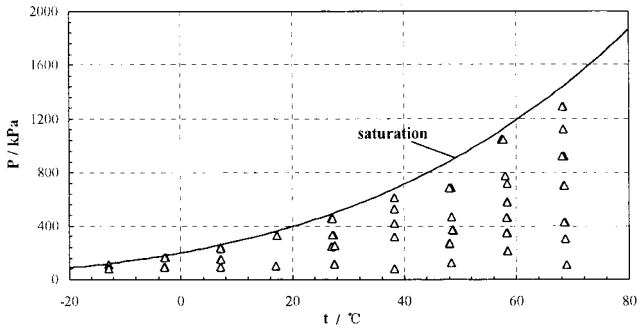

Figure 3. Temperature and pressure ranges for experimental points.

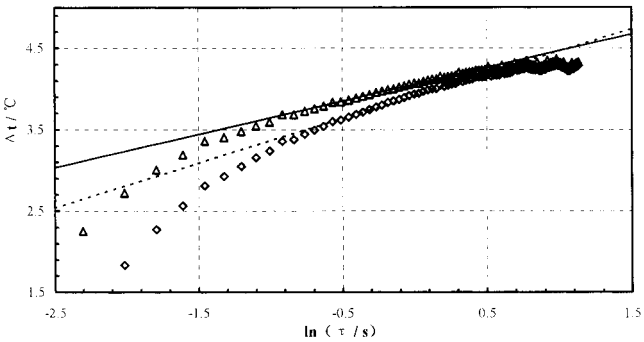

Figure 4. Temperature increase of the hot-wire and its linear function versus the logarithm time. ◇: Experimental data before correction; △: experimental data after correction; - - -: the linear function of experimental data before correction; —: the linear function of experimental data after correction.

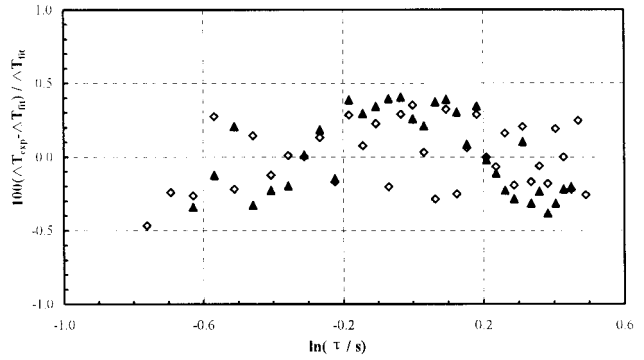

Figure 5. Deviation of temperature increase of the hot-wire from the linear correlation: ▲: Experimental data before correction; ◇: experimental data after correction.

nitrogen near the isotherm of 23.55 °C with values calculated from an equation recommended in the literature (Stephan et al., 1987). The pressure ranged from 436 to 2059 kPa. The recommended equation has an accuracy of ±0.8%. The mass purity of the nitrogen sample was 99.95%. The measured results deviated from the calculated values by a maximum deviation of less than 1% with a root mean square deviation of 0.42%. The results showed that the instrument was in a good condition and that the hot-wire method could be used to measure the thermal conductivity of fluids with a high accuracy. The author also used nitrogen to practice experimental steps and the skills to handle the experimental data.

Results and Analysis

The thermal conductivity of gaseous HFC-227ea was measured over the temperature range from 13.87 to 68.58 °C at pressures up to 1289 kPa. The mass purity of the

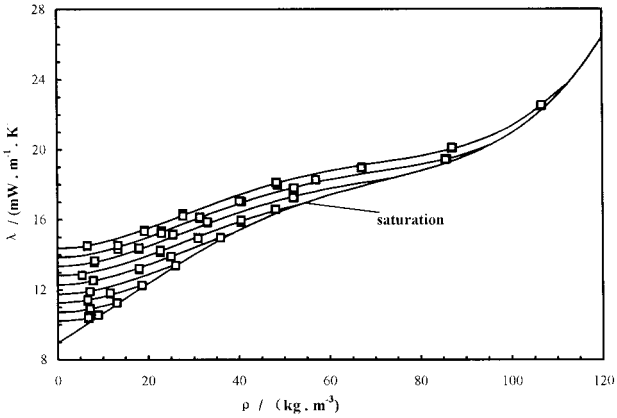

Figure 6. Thermal conductivity of gaseous HFC-227ea versus density near different isotherms. The temperatures of the isotherms are −13.81, −3.87; 6.80; 16.50; 27.40; 37.83; 48.40; 58.49; and 68.37 °C.

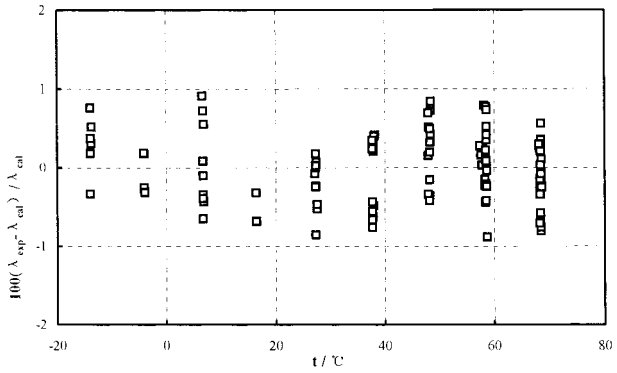

Figure 7. Deviations of the experimental thermal conductivity from eq 6.

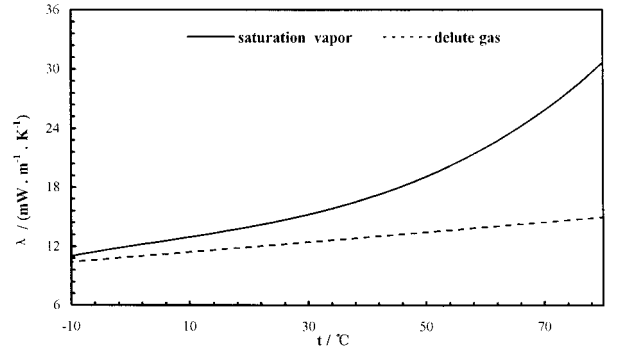

Figure 8. Thermal conductivity of saturated vapor and dilute gas of HFC-227ea.

HFC-227ea sample was 99.9%. The vapor densities were calculated using the Martin−Hou equation provided by Robin (1994). The specific heat at constant pressure was calculated by the database REFPROP.

Figure 3 shows the pressure range and temperature range of the experimental points. Figure 4 shows the temperature increase ΔT and DT_{id} versus the logarithm of time τ for a typical run using HFC-227ea. The data were correlated using a least-squares analysis. The relative deviations of the experimentally measured temperature increase from the linear function in Figure 4 are shown in Figure 5 for HFC-227ea in the conduction region. No curvature or systematic trend is apparent and the maximum deviation is less than ±0.5%. Similar plots were prepared for all of the measurements described in this paper. The lack of any curvature or systematic trend as

Table 1. Measured Thermal Conductivity of Gaseous HFC-227ea

t/°C	P/kPa	ρ/kg·m^{-3}	λ/mW·K^{-1}·m^{-1}	t/°C	P/kPa	ρ/kg·m^{-3}	λ/mW·K^{-1}·m^{-1}
−13.64	108.17	9.014	10.560	48.44	367.34	25.485	15.138
−13.71	108.17	9.017	10.534	48.45	367.94	25.529	15.148
−13.84	108.17	9.023	10.535	47.99	265.85	18.004	14.389
−13.87	83.52	6.875	10.347	47.99	266.45	18.047	14.315
−13.84	83.52	6.874	10.462	48.03	267.41	18.114	14.374
−13.86	83.52	6.875	10.401	48.21	125.18	8.193	13.558
−3.88	161.44	13.200	11.243	48.22	126.19	8.261	13.610
−3.94	161.44	13.205	11.247	48.22	127.04	8.318	13.653
−3.84	161.44	13.198	11.244	57.88	1045.60	85.595	19.458
−3.96	91.53	7.240	10.918	57.76	1045.42	85.931	19.452
−3.99	91.53	7.241	10.918	57.57	1045.58	85.805	19.431
6.94	233.09	18.693	12.227	57.77	1045.66	85.681	19.410
6.80	232.75	18.676	12.230	58.24	769.93	57.065	18.245
6.80	232.61	18.663	12.258	58.36	715.92	52.181	17.791
6.91	150.80	11.671	11.776	58.39	715.03	52.093	17.734
6.78	150.86	11.683	11.790	58.35	716.39	52.224	17.779
6.67	150.88	11.690	11.807	58.58	579.34	40.617	17.017
6.80	89.83	6.788	11.346	58.57	575.86	40.337	17.063
6.78	89.83	6.789	11.375	58.60	573.62	40.152	17.042
6.79	89.83	6.788	11.429	58.47	461.35	31.412	16.138
16.55	328.31	26.131	13.379	58.52	461.39	31.409	16.070
16.50	328.17	26.126	13.376	58.50	461.37	31.409	16.120
16.50	99.71	7.276	11.894	58.61	347.12	22.998	15.351
16.50	99.71	7.276	11.894	58.60	347.14	23.000	15.295
27.36	454.51	35.941	14.967	58.59	347.12	23.000	15.288
27.23	454.51	35.968	14.949	58.58	347.12	23.000	15.299
27.38	331.85	25.040	13.878	58.59	347.12	23.000	15.250
27.33	332.09	25.067	13.877	58.57	347.12	23.001	15.221
27.31	332.13	25.073	13.911	58.60	208.77	13.423	14.440
27.33	246.93	18.102	13.143	58.66	209.29	13.455	14.324
27.59	247.04	18.090	13.198	58.59	209.09	13.445	14.522
27.58	247.12	18.097	13.206	68.50	1288.76	106.580	22.458
27.46	113.36	7.968	12.529	68.50	1289.00	106.611	22.483
27.40	113.48	7.978	12.521	68.23	1289.00	106.862	22.504
27.35	113.56	7.985	12.538	68.50	1289.34	106.654	22.530
38.18	609.97	48.150	16.594	68.19	1119.99	87.208	20.076
37.99	609.97	48.205	16.586	68.38	1120.03	87.097	20.033
37.89	610.03	48.242	16.571	68.43	1119.97	87.056	20.100
37.99	529.05	40.557	15.837	68.29	919.13	67.203	18.958
37.89	528.75	40.553	15.941	68.37	918.67	67.127	18.980
37.85	528.75	40.561	15.959	68.47	918.51	67.074	18.940
37.84	419.37	30.991	14.926	68.43	704.41	48.643	17.948
37.71	419.35	31.011	14.951	68.40	701.75	48.436	18.110
37.70	419.45	31.020	14.917	68.43	699.97	48.285	18.115
37.65	316.84	22.694	14.254	68.39	700.83	48.362	18.102
37.70	316.84	22.694	14.125	68.48	427.21	27.718	16.337
37.81	316.86	22.695	14.238	68.13	426.63	27.715	16.276
37.69	81.59	5.480	12.824	68.22	426.99	27.731	16.185
48.23	684.08	52.245	17.249	68.30	303.88	19.247	15.372
47.97	683.12	52.232	17.239	68.22	303.86	19.251	15.383
48.14	682.36	52.108	17.225	68.23	303.84	19.249	15.313
48.34	464.85	33.136	15.808	68.41	109.51	6.688	14.527
48.36	464.75	33.125	15.824	68.58	109.50	6.683	14.495
48.35	464.55	33.110	15.870	68.45	109.47	6.684	14.513
48.47	366.82	25.442	15.123				

well as the small magnitude of the deviation indicates that no radiation correction is necessary for the temperature range considered (Nieto de Castro et al., 1991).

All of the results are given in Table 1. The thermal conductivity data were fit to the following equation

$$\lambda/\mathrm{mW\cdot m^{-1}\cdot K^{-1}} = a_0 + a_1(t/°\mathrm{C}) + b_2(\rho/\mathrm{kg\cdot m^{-3}})^2 + b_3(\rho/\mathrm{kg\cdot m^{-3}})^3 + b_4(\rho/\mathrm{kg\cdot m^{-3}})^4 \quad (9)$$

where $a_0 = 10.9104$, $a_1 = 5.04303 \times 10^{-2}$, $b_2 = 4.07168 \times 10^{-3}$, $b_3 = -6.80027 \times 10^{-5}$, and $b_4 = 3.42578 \times 10^{-7}$. The density of HFC-227ea was calculated by the Martin−Hou equation provided by Robin (1994). Figure 6 shows the thermal conductivity of gaseous HFC-227ea as a function of density near each isotherm. Figure 7 shows the deviations of the experimentally measured HFC-227ea thermal conductivity from eq 6, where λ_{exp} represents the experimental results and λ_{cal} are the values calculated from eq 6. The maximum deviation of the experimental results from eq 9 is 1.0%. The standard deviation of the experimental data from eq 9 is 0.44%.

Because eq 9 contains no linear density term, the effect of density on the thermal conductivity is greatly reduced close to the dilute gas state ($\rho \rightarrow 0$), in accordance with the kinetic theory of gases which states that the density effect should vanish at low densities. Equation 9 permits determination of the thermal conductivity of both superheated gas and gas at saturation conditions (Figure 6). For practical calculations, the thermal conductivity of saturated vapor as well as for the dilute gas is of special interest. The thermal conductivity for these conditions is plotted as functions of temperature in Figure 8. The results were extrapolated along isotherms because the density range did not extend to these two thermodynamic states. However,

the density range is wide enough for extrapolation and the errors caused by extrapolation are negligible. The thermal conductivity for saturated vapor λ'' can be extrapolated as

$$\lambda''/\mathrm{mW{\cdot}m^{-1}{\cdot}K^{-1}} = c_0 + c_1(t/°\mathrm{C}) + c_2(t/°\mathrm{C})^2 + c_3(t/°\mathrm{C})^3 \quad (10)$$

and the thermal conductivity for dilute gas λ_0 can be extrapolated as

$$\lambda_0/\mathrm{mW{\cdot}m^{-1}{\cdot}K^{-1}} = d_0 + d_1(t/°\mathrm{C}) \quad (11)$$

The coefficients c_i were determined to be $c_0 = 12.0081$, $c_1 = 9.33044 \times 10^{-2}$, $c_2 = -3.45433 \times 10^{-4}$, and $c_3 = 2.61499 \times 10^{-5}$. The coefficients d_i correspond to the coefficients a_i in eq 6. Figure 8 shows that λ'' and λ_0 are nearly equal at −10 °C, but begin to deviate as the temperature increases. This further indicates that both the temperature and density have an important effect on the thermal conductivity.

Conclusion

An instrument containing two hot-wires was carefully developed to measure the thermal conductivity of fluids. The thermal conductivity of gaseous HFC-227ea was measured from −13.87 to 68.58 °C at pressures up to 1289 kPa with an uncertainty of less than ±3%.

Literature Cited

Duan, Y. Y.; Sun, L. Q.; Shi, L.; Zhu, M. S.; Han, L. Z. Thermal Conductivity of Gaseous Trifluoroiodomethane (CF_3I). *J. Chem. Eng. Data* **1997**, *42*, 890−893.

Healy, J. J.; De Groot, J. J.; Kestin, J. The Theory of the Transient Hot-wire Method for Measuring Thermal Conductivity. *Physica* **1976**, *82C*, 392−408.

Huber, M.; Mclinden, M.; Gallagher, J. NIST Standard Reference Database 23: Thermodynamic properties of refrigerants and refrigerant mixtures database (RETPROP), version 5.0; U.S. Department of Commerce: Washington, DC, 1996.

Kestin, J.; Wakeham, W. A. A Contribution to the Theory of the Transient Hot-wire Technique for Thermal Conductivity Measurements. *Physica* **1978**, *92A*, 102−116.

Menashe, J.; Wakeham, W. A. Absolute Measurements of the Thermal Conductivity of Liquids at Pressures up to 500 MPa. *Phys. Chem.* **1981**, *85*, 340−347.

Nieto de Castro, C. A.; Perkins, R. A.; Roder, H. M. Radiative Heat Transfer in Transient Hot-wire Measurements of Thermal Conductivity. *Int. J. Thermophys.* **1991**, *12*, 985−997.

Jeschke, P. Thermal Conductivity of Refractories Working with the Hot-Wire Method. *Thermal Transmission Measurements of Insulation*; ASTM Special Technical Publication 660; American Society for Testing and Materials: Philadelphia, PA, **1977**; pp 172−185.

Robin, M. L. Thermophysical Properties of HFC-227ea. *Proceedings of 1994 International CFC & Halon Alternatives Conference*, Washington, DC: 1994; 105−113.

Salvi-Narkhede, M.; Wang, B. H.; Adcock, J. L.; Van Hook, W. A. Vapor Pressures, Liquid Molar Volumes, Vapor Non-ideality, and Critical Properties of some Partially Fluorinated Ethers ($CF_3OCF_2CF_2H$, CF_3OCF_2H, and CF_3OCH_3), some Perfluoroethers ($CF_3OCF_2OCF_3$, c-$CF_2OCF_2OCF_2$ and c-$CF_2CF_2CF_2O$) and of CHF_2Br and CF_3-$CFHCF_3$. *J. Chem. Thermodyn.* **1992,** *24*, 1065−1075.

Stephan, K.; Krauss, R.; Laesecke, A. Viscosity and Thermal Conductivity of Nitrogen for a Wide Range of Fluid States. *J. Phys. Chem. Ref. Data* **1987**, *16*(4), 993−1023.

Sun, L. Q.; Zhu, M. S.; Han, L. Z.; Lin, Z. Z. Thermal Conductivity of Gaseous Difluoromethane and Pentafluoroethane near the Saturation Line. *J. Chem. Eng. Data* **1997**, *42*, 179−182.

Received for review October 23, 1998. Accepted April 19, 1999. This work was supported by the National Natural Science Foundation of China (Grant No. 59706012).

JE9802625